Restoration of Na+/H+ exchanger NHE3-containing macrocomplexes ameliorates diabetes-associated fluid loss

Peijian He, *Emory University*
Luqing Zhao, *Emory University*
Lixin Zhu, *State University of New York, Buffalo*
Edward J. Weinman, *University of Maryland*
Roberto De Giorgio, *University of Bologna*
Michael Koval, *Emory University*
Shanthi Srinivasan, *Emory University*
Chang-Hyon Yun, *Emory University*

Journal Title: Journal of Clinical Investigation

Volume: Volume 125, Number 9

Publisher: American Society for Clinical Investigation | 2015-09-01, Pages 3519-3531

Type of Work: Article | Final Publisher PDF

Publisher DOI: 10.1172/JCI79552

Permanent URL: https://pid.emory.edu/ark:/25593/rgf5r

Final published version: http://dx.doi.org/10.1172/JCI79552

Restoration of Na^+/H^+ exchanger NHE3-containing macrocomplexes ameliorates diabetes-associated fluid loss

Peijian He,[1] Luqing Zhao,[1,2] Lixin Zhu,[3] Edward J. Weinman,[4] Roberto De Giorgio,[5] Michael Koval,[6] Shanthi Srinivasan,[1,7] and C. Chris Yun[1,7,8]

[1]Division of Digestive Diseases, Department of Medicine, Emory University School of Medicine, Atlanta, Georgia, USA. [2]Division of Gastroenterology, Department of Medicine, Beijing Hospital of Traditional Chinese Medicine affiliated with Capital Medical University, Beijing, China. [3]Digestive Diseases and Nutrition Center, Department of Pediatrics, State University of New York, Buffalo, New York, USA. [4]Division of Nephrology, Department of Medicine, University of Maryland School of Medicine, Baltimore, Maryland, USA. [5]Department of Medical and Surgical Sciences, University of Bologna; St. Orsola-Malpighi Hospital; and Centro Unificato di Ricerca Biomedica Applicata, Bologna, Italy. [6]Division of Pulmonary, Department of Medicine, Allergy, Critical Care and Sleep Medicine, Emory University School of Medicine, Atlanta, Georgia, USA. [7]Atlanta VA Medical Center, Decatur, Georgia, USA. [8]Winship Cancer Institute, Emory University School of Medicine, Atlanta, Georgia, USA.

Diarrhea is one of the troublesome complications of diabetes, and the underlying causes of this problem are complex. Here, we investigated whether altered electrolyte transport contributes to diabetic diarrhea. We found that the expression of Na^+/H^+ exchanger NHE3 and several scaffold proteins, including NHE3 regulatory factors (NHERFs), inositol trisphosphate (IP_3) receptor-binding protein released with IP_3 (IRBIT), and ezrin, was decreased in the intestinal brush border membrane (BBM) of mice with streptozotocin-induced diabetes. Treatment of diabetic mice with insulin restored intestinal NHE3 activity and fluid absorption. Molecular analysis revealed that NHE3, NHERF1, IRBIT, and ezrin form macrocomplexes, which are perturbed under diabetic conditions, and insulin administration reconstituted these macrocomplexes and restored NHE3 expression in the BBM. Silencing of NHERF1 or IRBIT prevented NHE3 trafficking to the BBM and insulin-dependent NHE3 activation. IRBIT facilitated the interaction of NHE3 with NHERF1 via protein kinase D2–dependent phosphorylation. Insulin stimulated ezrin phosphorylation, which enhanced the interaction of ezrin with NHERF1, IRBIT, and NHE3. Additionally, oral administration of lysophosphatidic acid (LPA) increased NHE3 activity and fluid absorption in diabetic mice via an insulin-independent pathway. Together, these findings indicate the importance of NHE3 in diabetic diarrhea and suggest LPA administration as a potential therapeutic strategy for management of diabetic diarrhea.

Introduction

Gastrointestinal complications, including gastroparesis, diarrhea, constipation, and fecal inconsistence, are common to patients with diabetes mellitus (DM). Diabetic diarrhea attains clinical significance because of its severity and refractory nature. The overall incidence of diabetic diarrhea can reach as high as 22% (1). Diabetic diarrhea occurs more frequently in young to middle-aged patients with poorly controlled insulin-requiring diabetes. These symptoms are often caused by autonomic neuropathy, bacterial overgrowth, bile acid malabsorption, electrolyte imbalance, and altered gut hormone production (2). So far, treatment of diabetic diarrhea relies mainly on conventional drugs that slow gastrointestinal transit, such as loperamide and diphenoxylate (1, 3), but the results are often disappointing (2). Antibiotic treatment is effective but only for some patients (4). These observations are in line with the fact that the underlying causes of diabetic diarrhea are multifactorial and complex. A previous study showed that intestinal mucosal absorption of fluid and electrolytes was markedly decreased in the ilea and colons of streptozotocin-induced (STZ-induced) diabetic rats (5), raising the possibility that altered regulation of ion transporters and/or channels contributes to diabetic diarrhea. However, there is not yet a causal relationship between a specific ion transporter(s) or channel(s) and the fluid dysregulation in diabetes.

Several ion transporters/channels, including Cl^-/HCO_3^- exchangers SLC26A6 (also known as PAT1) and SLC26A3 (also known as DRA), Na^+/H^+ exchanger 3 (NHE3), and cystic fibrosis transmembrane conductance regulator (CFTR), maintain electrolyte balance in the gastrointestinal tract (6). Mutations in the *DRA* gene are associated with congenital chloride diarrhea in humans, and deletion of the *Nhe3* gene causes diarrhea in mice (7, 8). Defects in CFTR, which mediates Cl^- secretion, cause thickened mucus and impaired digestive enzyme secretion (9). On the other hand, activation of CFTR by enterotoxins causes secretory diarrhea (10).

In this study, we show that intestinal fluid absorption is reduced in STZ-induced diabetic mice. This decrease was associated with reduced expression of NHE3 and its binding proteins at the brush border membrane (BBM). STZ and insulin showed opposite effects on the interaction of NHE3, ezrin, NHE3 regulatory factor 1 (NHERF1), and inositol trisphosphate (IP_3) receptor-binding protein released with IP_3 (IRBIT). This study highlights that the assembly of the macrocomplex forms the central focal point of dia-

Conflict of interest: The authors have declared that no conflict of interest exists.
Submitted: October 21, 2014; **Accepted:** June 25, 2015.
Reference information: *J Clin Invest*. 2015;125(9):3519–3531. doi:10.1172/JCI79552.

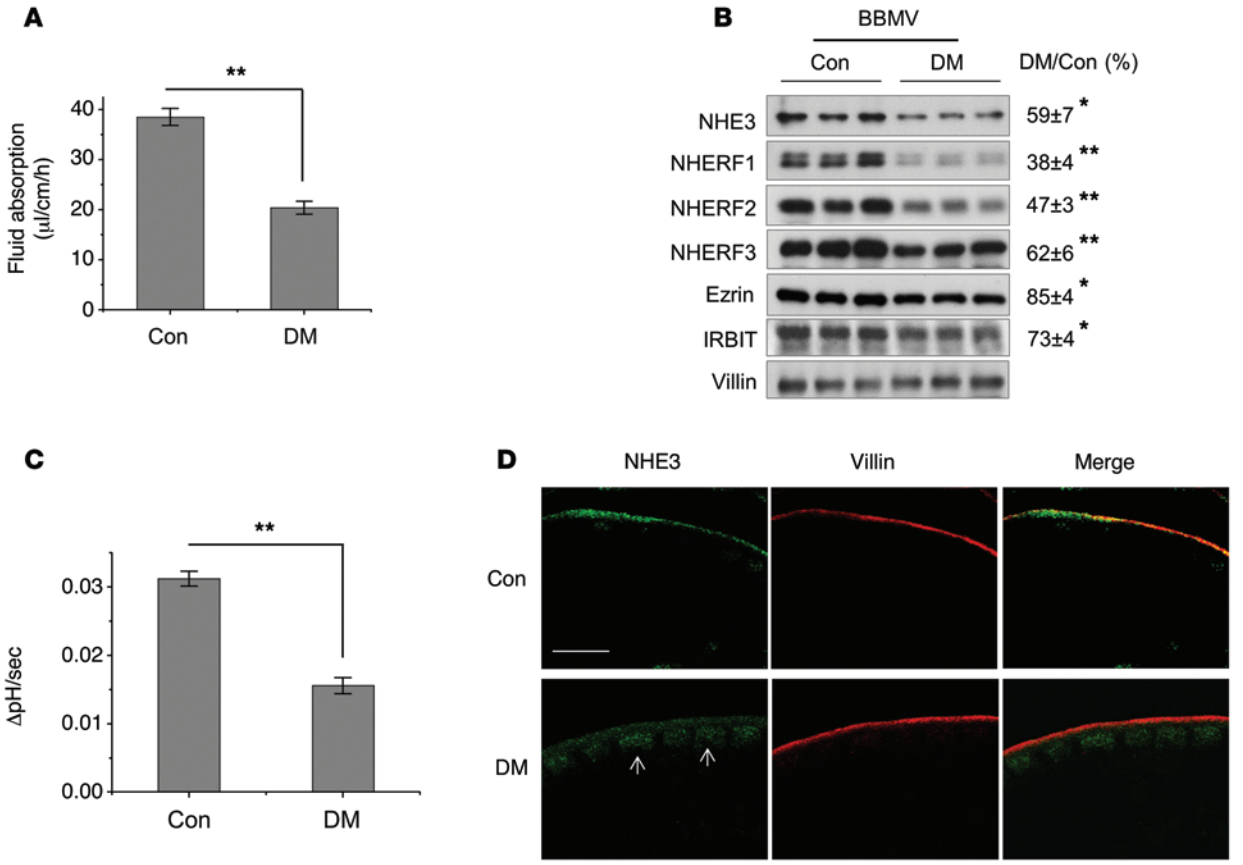

Figure 1. Fluid absorption and NHE3 activity in the ileum are reduced in diabetes. (**A**) Fluid absorption was measured for 2 hours in the ilea of control (Con) and T1DM (DM) mice. n = 5 mice per group. $^{**}P < 0.01$. (**B**) Protein expression in BBMVs of control and DM mice was determined. Villin was used as an internal marker of IECs. Protein expression levels (mean ± SEM) in DM mice relative to control mice are shown on the right. n = 6 per group. $^{*}P < 0.05$; $^{**}P < 0.01$. (**C**) NHE3 transport activity was determined in freshly isolated intestinal villi from control and DM mice in the presence of NHE1 and NHE2 inhibitor, Hoe-694 (40 μM). NHE3 activity is presented as the rate of Na^+-dependent pH change, ΔpHi/sec, at pH_i 6.5. n = 6. $^{**}P < 0.01$. (**D**) Representative confocal immunofluorescence images showing NHE3 (green) and villin (red) in ileal biopsies from patients with T1DM (n = 3) and controls (n = 2). Arrows show NHE3 expression in intracellular compartments. Scale bar: 10 μm. Statistical analysis was performed using 2-tailed Student's t test. Error bars indicate mean ± SEM.

betes-associated fluid loss. We also explored an alternative means to activate NHE3, hence mitigating fluid loss in diabetes.

Results

NHE3 activity and fluid absorption are decreased in the intestines of STZ-treated mice. Because clinical evidence supports the occurrence of intermittent diarrhea in many patients with type 1 DM (T1DM) (1), we used STZ-induced diabetes to model diabetes-associated diarrhea. Successful induction of diabetes in mice was demonstrated by hyperglycemia and weight reduction (Supplemental Table 1; supplemental material available online with this article; doi:10.1172/JCI79552DS1). However, there was no clear evidence of watery diarrhea over a period of 3 months of hyperglycemia. This was in contrast to an earlier report using rats, in which intermittent or persistent diarrhea was observed at 6 months of diabetes (5). We could not determine the water content of stool of diabetic mice, since stool and urine could not be separated. Nevertheless, DM mice had dilated intestines containing fluid, suggesting an impairment of net fluid absorption. To ascertain this possibility, we measured the net fluid absorption rate in the small intestine, a hallmark of diarrhea, by using an in vivo perfusion assay in which the net water movement was determined by using recirculating perfusion through an externalized intestinal loop (11). We found that the rate of fluid absorption was decreased by approximately 50% in the DM mice compared with that of controls (Figure 1A).

We reasoned that expression of ion transporters and channels that maintain intestinal fluid balance is altered in the DM mice. To this end, we analyzed the BBM vesicles (BBMVs) from the ilea of control and DM mice by proteomic analysis. The expression levels of DRA and CFTR were not significantly different between control and DM mice, although the signal intensity of these proteins was relatively low (Supplemental Figure 1A). Consistently, immunoblotting analysis showed no significant difference in BBM expression of CFTR protein between DM and control mice (Supplemental Figure 1B). PAT1 and NHE3 were not detected. The absence of NHE3 was unexpected since we observed over 20-fold enrichment of NHE3 in BBMVs (data not shown). Hence, we compared mRNA expression levels of these transporters in isolated intestinal epithelial cells (IECs) by RT-PCR. IECs from

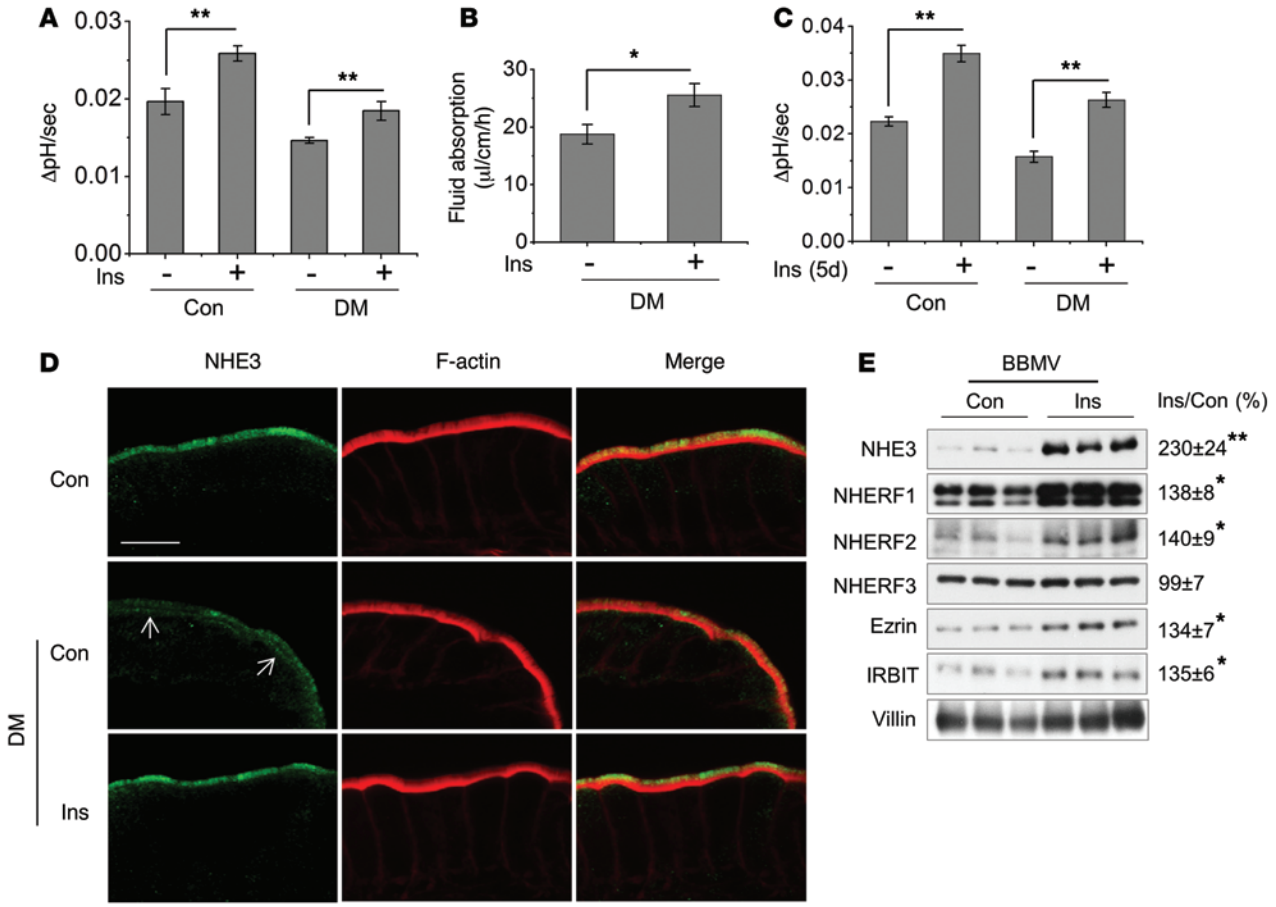

Figure 2. Insulin stimulates NHE3 activity and fluid absorption in the intestine. (**A**) Control and T1DM mice were treated with (+) or without (–) insulin for 30 minutes. NHE3 activity was determined in freshly isolated villi, and NHE3 activity is presented as the rate of Na^+-dependent pH change. $n = 5$ per group. $^{**}P < 0.01$. (**B**) DM mice were treated with or without insulin, and the rate of fluid absorption was determined 30 minutes later. $n = 5$. $^{*}P < 0.05$. (**C**) NHE3 activity was determined in control and DM mice that were treated with or without insulin for 5 consecutive days. $n = 5$. $^{**}P < 0.01$. (**D**) Representative confocal immunofluorescence images of 3 independent experiments showing NHE3 (green) and F-actin (red) in mouse ileum. DM mice were treated with or without insulin for 30 minutes. Scale bar: 10 μm. Arrows point to NHE3 in the terminal web. (**E**) Protein expression was determined in BBMVs purified from DM mice that were treated with or without insulin for 30 minutes. Villin was used as an internal marker of IECs. Protein expression levels (mean ± SEM) in insulin-treated mice relative to controls are shown on the right. $n = 6$. $^{*}P < 0.05$; $^{**}P < 0.01$. Statistical analysis was performed using 2-tailed Student's *t* test. Error bars indicate mean ± SEM.

DM mice showed a significant decrease in *Nhe3* mRNA expression, but *Dra* or *Cftr* mRNA expression was not altered (Supplemental Figure 1C). *Pat1* mRNA was slightly elevated but did not reach statistical significance. Consistent with the decreased *Nhe3* mRNA expression, NHE3 protein expression in DM mice was reduced by approximately 25% (Supplemental Figure 1D).

Although we could not find significant changes in ion transporter and channel expression by proteomic analysis, the same proteomic analysis revealed that the expression levels of ezrin and NHERF1–NHERF3 were substantially lower in DM mouse intestines (Supplemental Figure 1A). Ezrin and NHERFs interact with NHE3, although their interaction is not exclusive (12). Western blot of BBMVs corroborated decreased expression of NHERF1–NHERF3 and ezrin (Figure 1B). In addition, decreased expression of NHE3 and the recently identified NHE3-binding partner IRBIT (13) in DM BBMVs was evident. Additionally, decreased NHE3 expression was paralleled by an approximately 50% decrease in NHE3 transport activity in isolated villi (Figure 1C). Of note, NHE3 activity was measured in the presence of 40 μM Hoe-694 that inhibits NHE1 and NHE2. We next asked whether the membrane expression of NHE3 is also altered in the ilea of patients with type 1 diabetes (Supplemental Table 2). Representative immunofluorescence staining revealed that, in contrast to the microvillus localization of NHE3 in control ileum, luminal membrane expression of NHE3 was decreased in DM biopsies (Figure 1D). In addition, a substantial portion of NHE3 was localized in intracellular compartments in DM.

Insulin enhances intestinal NHE3 activity and fluid absorption in diabetes. To determine whether decreased NHE3 activity in STZ-treated mice is due to the absence of insulin, we treated mice with insulin. Blood glucose levels in DM mice were reduced by 27% by acute (30-minute) insulin treatment (Supplemental Table 3), while there was no change in control mice. As shown in Figure 2A, insulin acutely increased NHE3 activity in both control and DM mice, consistent with previous reports that insulin stimulates NHE3 activity in renal proximal tubule cells (14, 15). NHE3 activ-

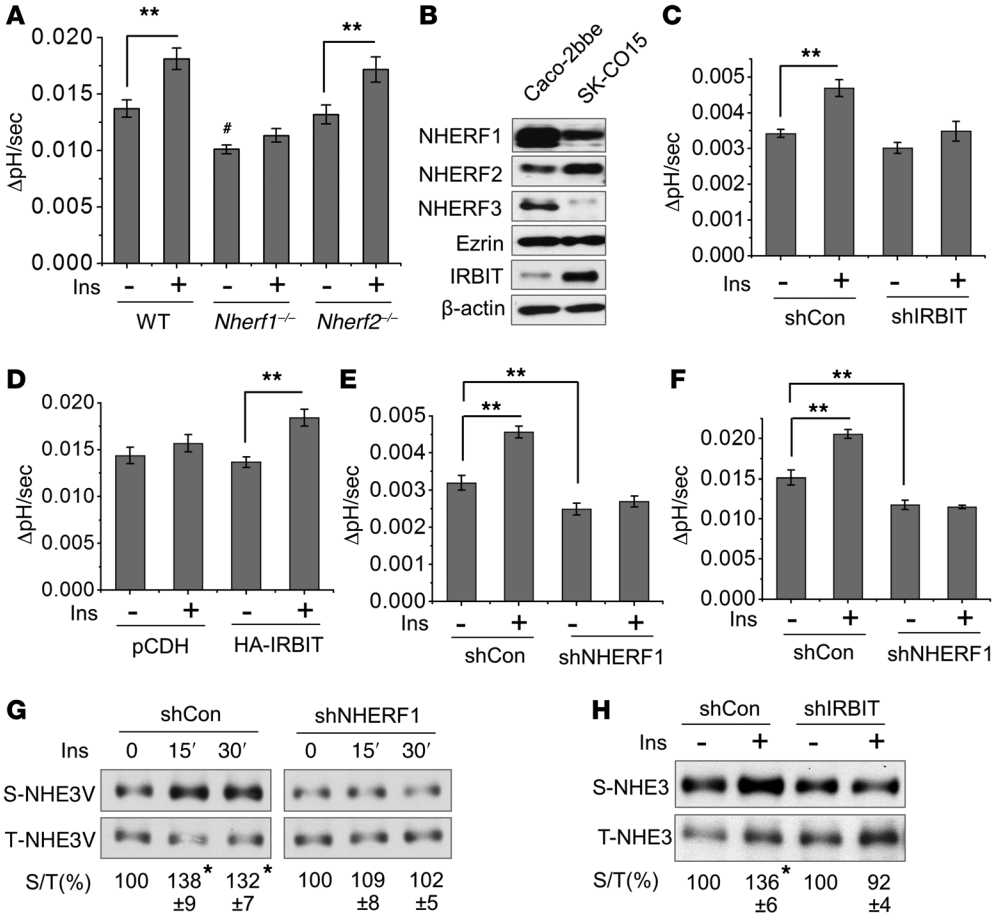

Figure 3. Activation of NHE3 by insulin requires NHERF1 and IRBIT. (**A**) WT, *Nherf1*$^{-/-}$, and *Nherf2*$^{-/-}$ mice were treated with or without insulin for 30 minutes. NHE3 activity was determined in isolated villi. n = 4 mice for each genotype. $^{**}P < 0.01$; $^{\#}P < 0.01$ compared with WT without insulin. (**B**) Expression of NHE3-binding proteins in Caco-2bbe and SK-CO15 cells. β-Actin was used as an internal control. n = 3. (**C**) NHE3 activity was measured in SK-CO15 cells transfected with control shRNA (shCon) or shRNA for IRBIT (shIRBIT). n = 8. $^{**}P < 0.01$. (**D**) NHE3 activity was measured in Caco-2bbe/NHE3V cells stably transfected with an empty vector pCDH or pCDH/HA-IRBIT (HA-IRBIT). n = 8. $^{**}P < 0.01$. NHE3 activity was determined in (**E**) SK-CO15 and (**F**) Caco-2bbe/NHE3V/HA-IRBIT cells transduced with shCon or shNHERF1. n = 8. $^{**}P < 0.01$. (**G**) Surface expression of NHE3 was determined in Caco-2bbe/NHE3V/HA-IRBIT cells with NHERF1 knockdown. The amount of surface (S) NHE3 was normalized to total (T) NHE3, and the relative changes are shown. n = 3. $^{*}P < 0.05$ compared with untreated control. (**H**) NHE3 surface expression was determined in SK-CO15 cells with IRBIT knockdown. n = 3. $^{*}P < 0.05$ compared with untreated control. Statistical analysis was performed using 2-tailed Student's t test. Error bars indicate mean ± SEM.

ity in insulin-treated DM mice was comparable to that in control mice, demonstrating that insulin is able to restore NHE3 activity to the normal physiological level. Moreover, acute insulin treatment significantly increased intestinal fluid absorption in DM mice (Figure 2B). In order to mimic insulin treatment of patients with T1DM, we administered insulin for 5 days, which lowered blood glucose by 36% in DM mice (Supplemental Table 3). Similar to the effect after acute insulin treatment, chronic insulin increased NHE3 activity in both control and DM mice (Figure 2C). The relative change in NHE3 activity was greater after 5 days of insulin compared with that after acute insulin treatment.

Trafficking of NHE3 in and out of the apical membrane is an important mechanism regulating NHE3 activity (16). We hence evaluated whether the subcellular localization of NHE3 is altered in DM mouse intestine. NHE3 is normally distributed along the microvilli above the terminal web marked by prominent staining of F-actin. However, in DM mice microvillous expression of NHE3 was reduced and a substantial fraction of NHE3 was found at the terminal web (Figure 2D). Importantly, insulin reconstituted NHE3 expression at the microvilli of DM intestine (Figure 2D). This result was corroborated by increased NHE3 expression in the BBM fraction from DM mice treated with insulin for 30 minutes (Figure 2E) or 5 days (Supplemental Figure 2A). Moreover, insulin also increased BBM expression of NHERF1, NHERF2, ezrin, and IRBIT, although NHERF3 expression was not altered. Notably, a 5-day of insulin treatment increased total NHE3 protein abundance without changing expression levels of NHE3 scaffold proteins (Supplemental Figure 2B). These results suggest that insulin restores the fluid absorption process in diabetes in part by the restoration of NHE3 expression and BBM localization. In the subsequent studies in which we elucidate the underlying mechanisms by which insulin regulates NHE3, mice and cells were acutely treated with insulin unless otherwise noted.

Insulin-induced activation of NHE3 is dependent on IRBIT and NHERF1. A question remains as to how insulin redistributes NHE3 to BBM. We contemplated whether the trafficking of NHE3 by insulin is dependent on the scaffold proteins that are altered in DM mice. We hypothesized that NHERF1, NHERF2, ezrin, or IRBIT might be involved in insulin-induced trafficking of NHE3. We ruled out NHERF3 based on the lack of effect on NHERF3 expression by insulin (Figure 2E). To examine the potential role of NHERF1 and NHERF2 in insulin-mediated NHE3 activation, we determined whether insulin activates NHE3 activity in mice lacking NHERF1 or NHERF2. NHE3 activity was significantly upregulated by acute insulin treatment in WT and NHERF2 KO (*Nherf2*$^{-/-}$) mice (Figure 3A). In contrast, the stimulatory effect of insulin was not observed in *Nherf1*$^{-/-}$ mice, indicating that NHERF1 is required for NHE3 activation. In Supplemental Figure 2B, we show that NHE3

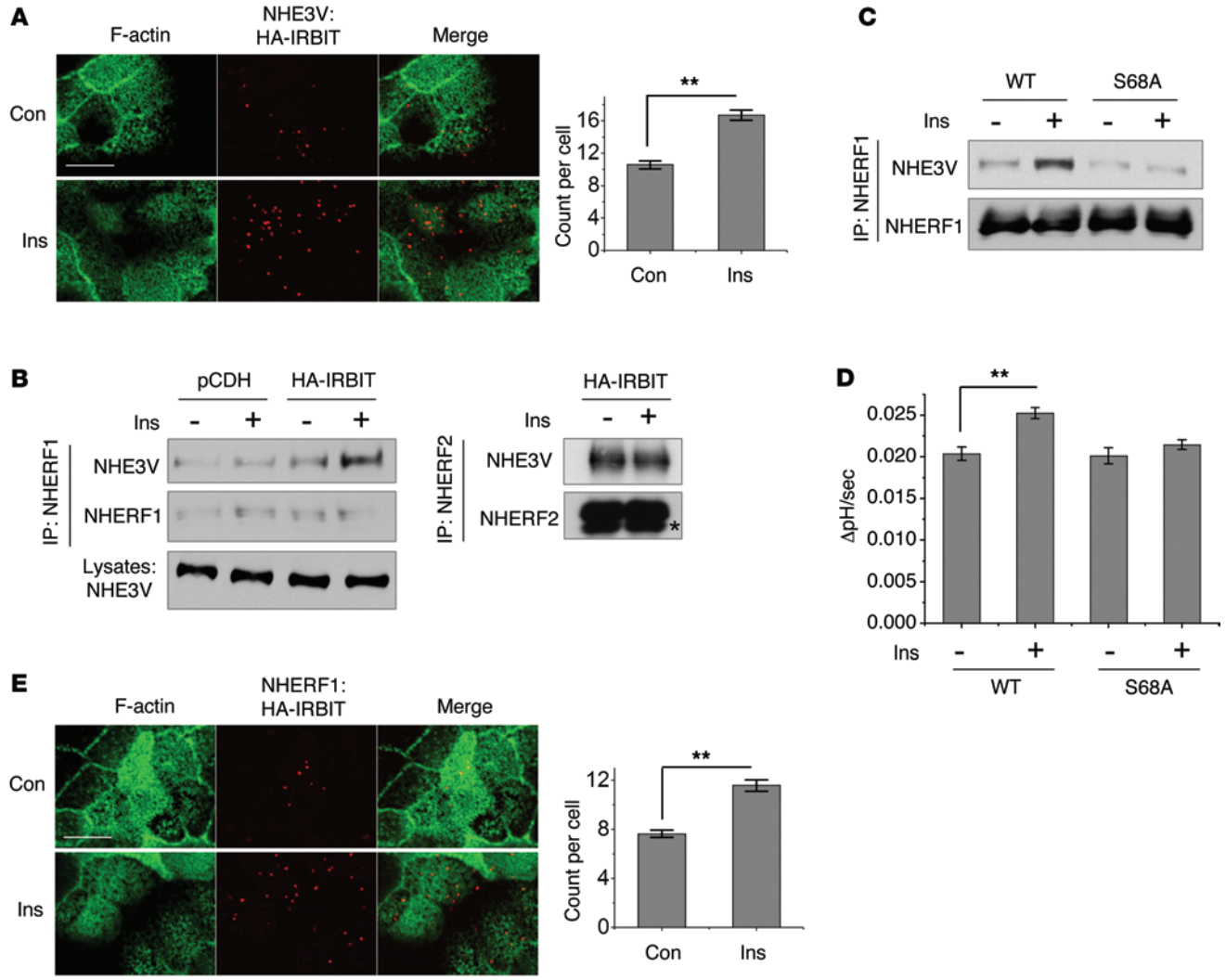

Figure 4. IRBIT facilitates the interaction between NHE3 and NHERF1. (**A**) Caco-2bbe/NHE3V/HA-IRBIT cells were treated with or without insulin for 15 minutes. The interaction between NHE3V and HA-IRBIT was determined by in situ PLA using mouse anti-VSVG and rabbit anti-HA antibodies. Interaction was indicated as red dots, and F-actin stained with Alexa Fluor 488 phalloidin is shown in green. Scale bar: 10 μm. Representative images of 3 independent experiments are shown. The number of red puncta (mean ± SEM) was counted from >50 representative cells, and the results are shown. $^{**}P < 0.01$. The NHERF1-NHE3 interaction was determined in Caco-2bbe/NHE3V cells expressing (**B**) control vector pCDH or HA-IRBIT and (**C**) WT or mutant (S68A) HA-IRBIT. The NHERF2-NHE3 interaction in response to insulin was determined in cells expressing HA-IRBIT. The asterisk denotes the band representing the total amount of immunoprecipitated NHERF2. Cells were treated with insulin for 15 minutes. $n = 3$. (**D**) Caco-2bbe/NHE3V cells expressing WT or S68A mutant HA-IRBIT were treated with or without insulin for 30 minutes, and NHE3 activity was determined. $n = 6$ for each group. $^{**}P < 0.01$. (**E**) The interaction between NHERF1 and HA-IRBIT was determined by PLA using rabbit anti-NHERF1 and mouse anti-HA antibodies. Scale bar: 10 μm. $^{**}P < 0.01$. $n = 3$. Statistical analysis was performed using 2-tailed Student's *t* test. Error bars indicate mean ± SEM.

expression was increased after 5 days of insulin treatment. Hence, we determined whether NHE3 activity is altered independent of NHERF1 by 5-day insulin treatment. We observed a 31% increase in NHE3 activity in *Nherf1*$^{-/-}$ mice compared with a 47% increase in WT mice, indicating that NHE3 regulation by chronic insulin treatment is partially dependent on transcriptional/translational activation of NHE3 (Supplemental Figure 3). However, the basal NHE3 activity was reduced in *Nherf1*$^{-/-}$ mice, as previously reported (17), which therein indicates that NHE3 activity in *Nherf1*$^{-/-}$ mice after 5 days of insulin treatment was significantly lower compared with that of WT mice.

IRBIT mediates the NHE3-NHERF1 interaction. Because the IRBIT-NHE3 interaction is dynamically regulated by angiotensin II in renal proximal tubular epithelial cells (19), we hypothesized that insulin enhances the interaction of IRBIT with NHE3 in IECs. To this end, we used in situ proximity ligation assay (PLA), which results in a fluorescent signal when two proteins interact. As shown in Figure 4A, the NHE3-IRBIT interaction occurred in the apical membrane domain under basal conditions, as evidenced by the presence of red fluorescence signal. Importantly, insulin increased the number of red fluorescence puncta, indicating that it enhances the NHE3-IRBIT interaction. NHERF1 was initially identified as an NHE3-binding protein (20). Hence, we examined whether the NHERF1 and NHE3 interaction is altered in response to insulin. NHERF1 coimmunoprecipitated NHE3 in Caco-2bbe cells under basal conditions,

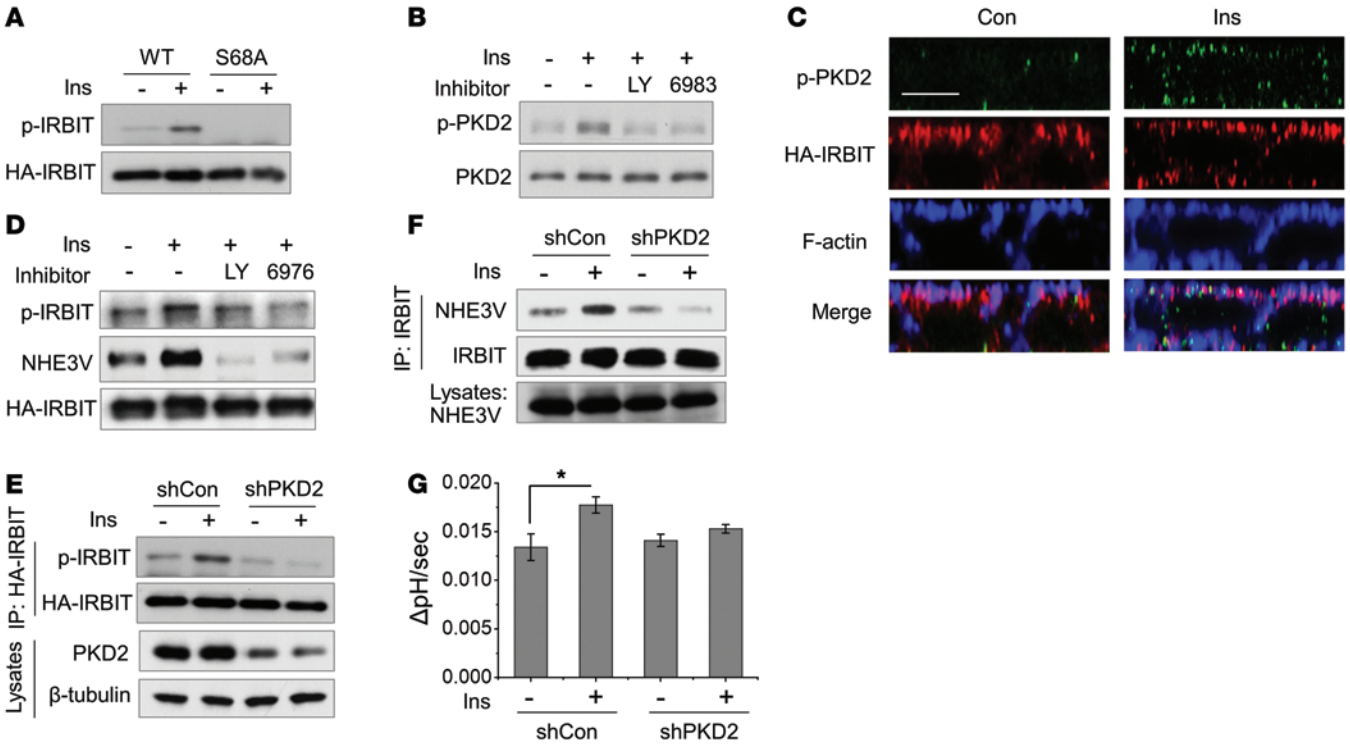

Figure 5. PKD2 mediates IRBIT phosphorylation and NHE3 activation. (**A**) Caco-2bbe/NHE3V cells expressing WT or S68A mutant HA-IRBIT were treated with or without insulin for 15 minutes. HA-IRBIT was immunoprecipitated with anti-HA antibody, and phosphorylation of IRBIT was determined using anti–phospho-Ser antibody. Representative blots of 3 independent experiments are shown. (**B**) Caco-2bbe cells were pretreated with 20 μM LY294002 (LY) or 5 μM Gö6983 (6983). Phosphorylation of PKD2 (p-PKD2) was examined in response to insulin treatment for 15 minutes. $n = 3$. (**C**) Cellular localization of p-PKD2 (green) and IRBIT (red) in Caco-2bbe/NHE3V/HA-IRBIT cells was analyzed by confocal microscopy. F-actin (blue) was used as a marker of the apical compartment of the cells. Scale bar: 10 μm. $n = 3$. (**D**) Caco-2bbe/NHE3V/HA-IRBIT cells were pretreated with 20 μM LY294002 or 2 μM Gö6976. HA-IRBIT was immunoprecipitated, and phosphorylation of IRBIT was determined. The amount of NHE3 coimmunoprecipitated was determined with anti-VSVG antibody. $n = 3$. (**E**) Phosphorylation of IRBIT in response to insulin was determined in PKD2 knockdown (shPKD2) and control cells. Expression of PKD2 and β-tubulin in cell lysates is shown. $n = 3$. (**F**) The IRBIT-NHE3 interaction was examined in Caco-2bbe/NHE3V/HA-IRBIT cells transfected with shPKD2 or shCon. $n = 3$. (**G**) NHE3 activity was determined in Caco-2bbe/NHE3V/HA-IRBIT cells with stable knockdown of PKD2. $n = 6$. $^*P < 0.05$, 2-tailed Student's t test. Error bars indicate mean ± SEM.

but their interaction was marginally enhanced by insulin (Figure 4B, left panels). Because we showed above (Figure 3) that insulin failed to regulate NHE3 unless IRBIT was overexpressed, we assessed whether IRBIT influences the NHE3-NHERF1 interaction. Exogenous expression of HA-IRBIT increased the efficiency of NHE3 coimmunoprecipitation with NHERF1 under basal conditions, which was further enhanced by insulin (Figure 4B). In contrast, the interaction between NHE3 and NHERF2 was not altered by insulin (Figure 4B). In silico analysis of the IRBIT sequence has identified Ser68 as a potential phosphorylation site by CaMKII or protein kinase D (PKD) family kinases (PKD1–PKD3) (21). Phosphorylation of IRBIT at Ser68 is essential for its binding and regulation of its target proteins, including NHE3, IP_3 receptor, and Na^+-HCO_3^- cotransporter 1 (13, 22, 23). To further confirm the role of IRBIT in the NHERF1-NHE3 interaction, we used IRBIT with Ser68 altered to Ala (S68A), which is incapable of binding NHE3 (19). In contrast to WT IRBIT, IRBIT-S68A failed to recapitulate the stimulatory effect on the NHE3-NHERF1 interaction by insulin (Figure 4C). Moreover, in the absence of the enhanced NHE3-NHERF1 association, insulin did not regulate NHE3 activity (Figure 4D). These results imply that IRBIT may interact with NHERF1 to facilitate NHE3-NHERF1 association. To gain evidence for the direct interaction between IRBIT and NHERF1, we used PLA again. As shown in Figure 4E, insulin increased the proximity signal between IRBIT and NHERF1 in the apical membrane domain. These results collectively suggest that IRBIT facilitates the association of NHERF1 with NHE3.

Activation of NHE3 by insulin depends on IRBIT phosphorylation by PKD2. Given the importance of Ser68 phosphorylation in the interaction of IRBIT with NHE3 and NHERF1, we investigated whether insulin induces IRBIT phosphorylation in Caco-2bbe cells by determining the phosphorylation level of immunoprecipitated HA-IRBIT using anti–phospho-Ser antibody. We found that insulin enhanced phosphorylation of WT HA-IRBIT, but not HA-IRBIT-S68A (Figure 5A), demonstrating that Ser68 is phosphorylated by insulin-mediated signal. PKD is a downstream target of PKC (24), which can be activated by insulin (25). Hence, we investigated whether insulin increases IRBIT phosphorylation through PKD. We focused on PKD2 because PKD2 is the dominant form of PKD in IECs (26). Insulin treatment resulted in a marked increase of PKD2 phosphorylation at Ser876

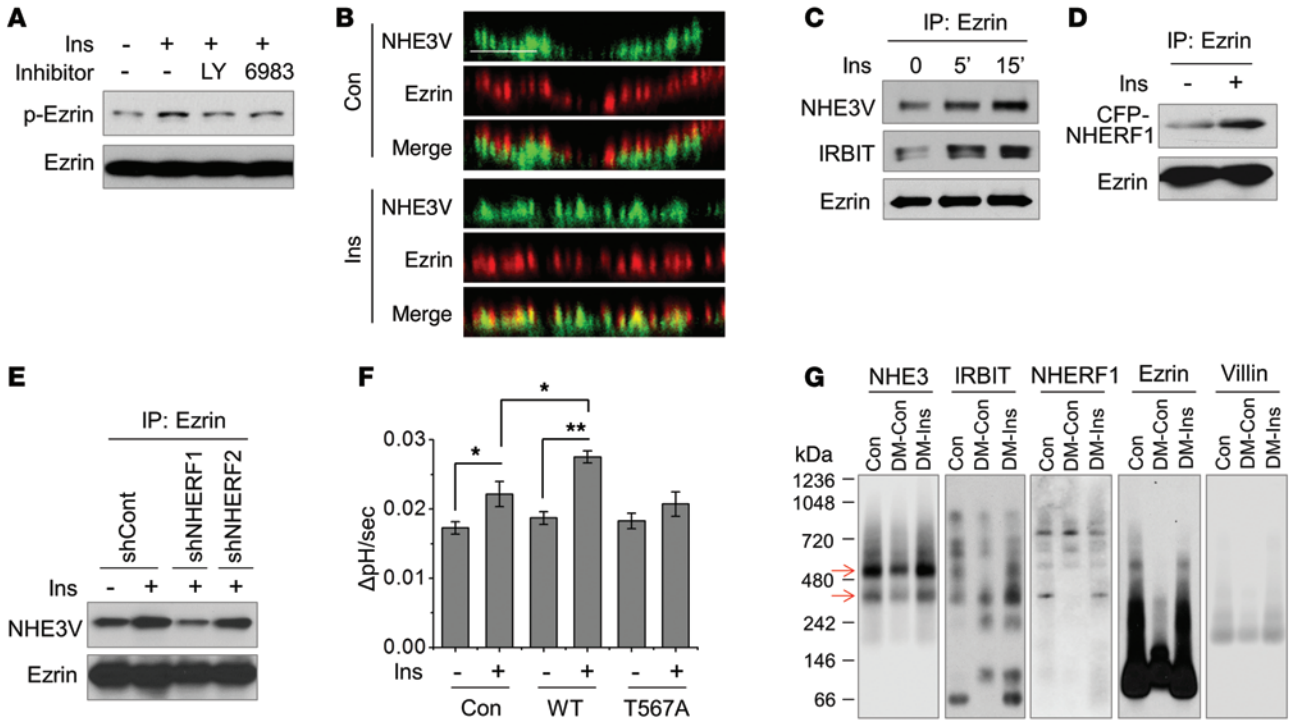

Figure 6. Ezrin assembles with NHERF1, IRBIT, and NHE3 in macromolecular complexes and mediates NHE3 activation by insulin. (**A**) Phosphorylation of ezrin at Thr567 (p-Ezrin) was examined in Caco-2bbe/NHE3V/HA-IRBIT cells. Cells were pretreated with or without 20 μM LY294002 or 5 μM Gö6983, followed by insulin treatment for 15 minutes. $n = 4$. (**B**) Subcellular localization of NHE3 (green) and ezrin (red) in the apical zone (3 μm) of Caco-2bbe/NHE3V/HA-IRBIT cells. Scale bar: 10 μm. Representative images of 3 independent experiments are shown. (**C**) The interaction of ezrin with NHE3 and IRBIT was examined in Caco-2bbe/NHE3V/HA-IRBIT cells in the presence of a cross-linker, dithiobis(succinimidyl propionate) (DSP). $n = 3$. (**D**) The ezrin-NHERF1 interaction was examined in Caco-2bbe/NHE3V/HA-IRBIT cells expressing CFP-NHERF1. $n = 4$. (**E**) The effects of NHERF1 and NHERF2 knockdown on the ezrin-NHE3 interaction were determined in Caco-2bbe/NHE3V/HA-IRBIT cells. $n = 4$. (**F**) NHE3 activity (mean ± SEM) was determined in Caco-2bbe/NHE3V/HA-IRBIT cells expressing WT or mutant (T567A) CFP-ezrin. $n = 6$. $^*P < 0.05$; $^{**}P < 0.01$, 2-tailed Student's t test. Error bars indicate mean ± SEM. (**G**) BBMVs of control and DM mice treated with or without insulin for 30 minutes were resolved by BN-PAGE. Expression of NHE3, IRBIT, NHERF1, and ezrin is shown. Villin was used as a marker of BBM. Arrows indicate the macrocomplexes containing NHE3. Representative blots of 3 independent experiments are shown.

(active form of PKD2), which was blocked by either the PI3K inhibitor LY294002 or PKC inhibitor Gö6983 (Figure 5B). Confocal immunofluorescence analysis showed that phospho-PDK2 abundance was enhanced by insulin at the apical membrane where it colocalized with IRBIT (Figure 5C). Moreover, insulin-mediated IRBIT phosphorylation was blocked by pretreating the cells with LY294002 or Gö6976, an inhibitor of PKC and PKD, and notably, the amount of NHE3 protein coimmunoprecipitated correlated with the phosphorylation level of IRBIT (Figure 5D). Insulin-mediated phosphorylation of IRBIT was abolished by PKD2 knockdown (Figure 5E), further asserting the role of PKD2 in IRBIT phosphorylation. Not surprisingly, knockdown of PKD2 mitigated the increase in NHE3-IRBIT binding (Figure 5F) and NHE3 activity by insulin (Figure 5G), demonstrating that PKD2 regulates NHE3 activity by enhancing the NHE3-IRBIT interaction. It has been shown that phosphorylation of NHERF1 by PKC results in dissociation of NHERF1 from an interacting protein (27). Because insulin-mediated NHE3 regulation involves PKC, we determined whether NHERF1 is phosphorylated by insulin. However, we could not detect NHERF1 phosphorylation by insulin (Supplemental Figure 4), indicating that insulin-mediated NHE3 regulation does not involve NHERF1 phosphorylation.

Activation of NHE3 by insulin requires the assembly of ezrin-NHERF1-IRBIT-NHE3 complex. Ezrin functions as a linker between the plasma membrane and cytoskeleton and mediates mobilization of membrane proteins (28). Phosphorylation of ezrin at Thr567 activates ezrin by relieving the self-association between the N- and C-termini of ezrin (29). We observed that insulin acutely increased phosphorylation of ezrin at Thr567, which was blocked by inhibition of PI3K or PKC (Figure 6A). Because our study above showed that insulin restored the altered BBM expression of ezrin and NHE3 in DM mouse intestine, we sought to determine whether insulin regulates the ezrin and NHE3 interaction. As shown in Figure 6B, NHE3 was located below ezrin in resting cells, and insulin promoted NHE3 translocation toward the apical membrane, resulting in colocalization of NHE3 with ezrin. The insulin-induced interaction of NHE3 with ezrin was confirmed by coimmunoprecipitation, in which an increased amount of NHE3 was detected in ezrin-bound immunocomplex (Figure 6C). Moreover, insulin promoted the interaction of ezrin with IRBIT. Because the MW of NHERF1 is close to IgG, we expressed CFP-NHERF1 in Caco-2bbe cells to determine the interaction of NHERF1 with ezrin. Our results show that insulin acutely enhanced the association of CFP-NHERF1 with ezrin (Figure 6D).

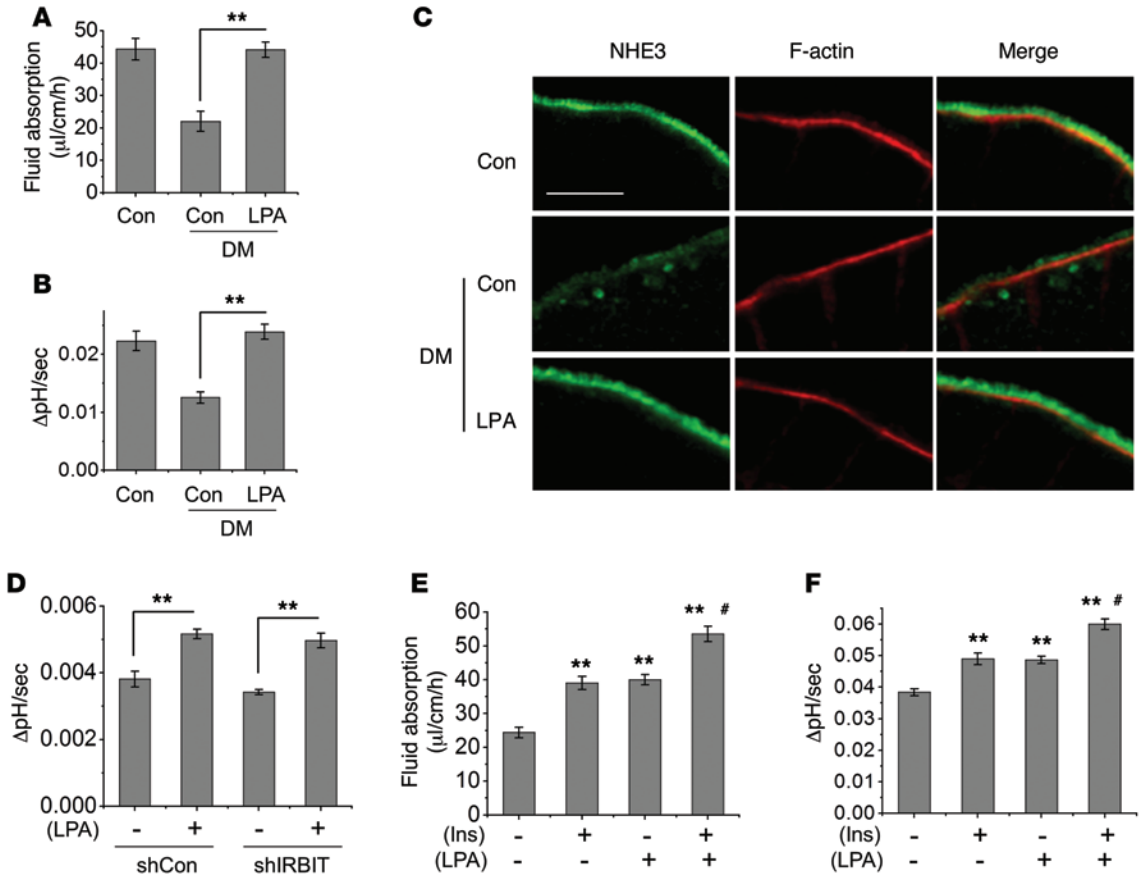

Figure 7. LPA activates NHE3 and fluid absorption in the intestines of DM mice. (**A**) Fluid absorption and (**B**) NHE3 activity were determined with control and DM mice. Where indicated, DM mice received LPA (20 μM) or PBS (Con) orally for 5 days. $n = 5$ mice per group. $^{**}P < 0.01$. (**C**) Representative immunofluorescence images of 5 independent experiments showing NHE3 (green) and F-actin (red) in mouse ileum. Scale bar: 10 μm. (**D**) NHE3 activity was determined in SK-CO15/HA-LPA5 cells with stable IRBIT knockdown. Cells were treated with 1 μM LPA for 30 minutes. $n = 6$. $^{**}P < 0.01$. (**E**) Fluid absorption was determined in DM mice treated with or without insulin, LPA, or insulin plus LPA for 5 days. $n = 5$ mice per group. $^{**}P < 0.01$ compared with untreated control; $^{\#}P < 0.01$ compared with insulin or LPA alone. (**F**) Caco-2bbe/NHE3V/HA-IRBIT cells expressing LPA5 were treated with insulin, LPA, or insulin plus LPA for 30 minutes. NHE3 activity was compared. $^{**}P < 0.01$ compared with untreated control; $^{\#}P < 0.01$ compared with insulin or LPA alone. $n = 6$. Statistical analysis was performed using 2-tailed Student's t test. Error bars indicate mean ± SEM.

Because ezrin also binds NHE3 indirectly via NHERF1 or NHERF2 (30), we determined whether the insulin-induced increase in ezrin-NHE3 interaction was dependent on NHERF1 or NHERF2. Knockdown of NHERF2 (>80%) did not affect coimmunoprecipitation of ezrin and NHE3 (Figure 6E), consistent with the data in Figure 3A that insulin activated NHE3 in *Nherf2*$^{-/-}$ mice. In contrast, depletion of NHERF1 markedly decreased coimmunoprecipitation of NHE3 by ezrin, supporting the importance of NHERF1 for the NHE3-ezrin interaction. To determine the functional importance of ezrin in NHE3 regulation, CFP-tagged WT ezrin or inactive ezrin-T567A was expressed in Caco-2bbe/NHE3V/HA-IRBIT cells. As shown in Figure 6F, unlike that in CFP-ezrin–transfected cells, insulin failed to activate NHE3 in cells expressing CFP-ezrin-T567A, indicating the necessity of ezrin activation in the regulation of NHE3.

The above findings suggested that interactions among ezrin, NHERF1, IRBIT and NHE3 form the structural basis of NHE3 regulation by insulin. To further test this idea, we resolved BBMVs from the intestine of DM and control mice by blue native–PAGE (BN-PAGE). In control BBMs, NHE3 was mainly present in 2 large macrocomplexes, with approximate sizes of 400 kDa and 550 kDa (Figure 6G). Western blotting showed that both of these complexes contained ezrin, IRBIT, and NHERF1. However, in DM mice, we found that IRBIT was absent in the 550-kDa complex, while the 400-kDa complex lacked NHERF1. Ezrin was absent in both macrocomplexes. Strikingly, acute insulin treatment of DM mice reconstituted the expression of IRBIT, NHERF1, and ezrin in these macrocomplexes (Figure 6G), verifying that the absence of the multiprotein complexes correlates with diabetic conditions.

Lysophosphatidic acid enhances intestinal Na^+ and fluid absorption independent of insulin. Lysophosphatidic acid (LPA) is a growth factor–like lipid molecule that mediates multiple biological effects through 6 LPA receptors (31). We have shown previously that LPA activates NHE3 via the LPA5 receptor in Caco-2bbe cells and mouse ileum (11, 32). The activation of NHE3 by LPA is independent of PI3K and is regulated by the ERK-RSK2 cascade (33), suggesting that LPA and insulin might regulate NHE3 through different pathways. Hence, we investigated whether LPA can restore NHE3 activity and fluid homeostasis

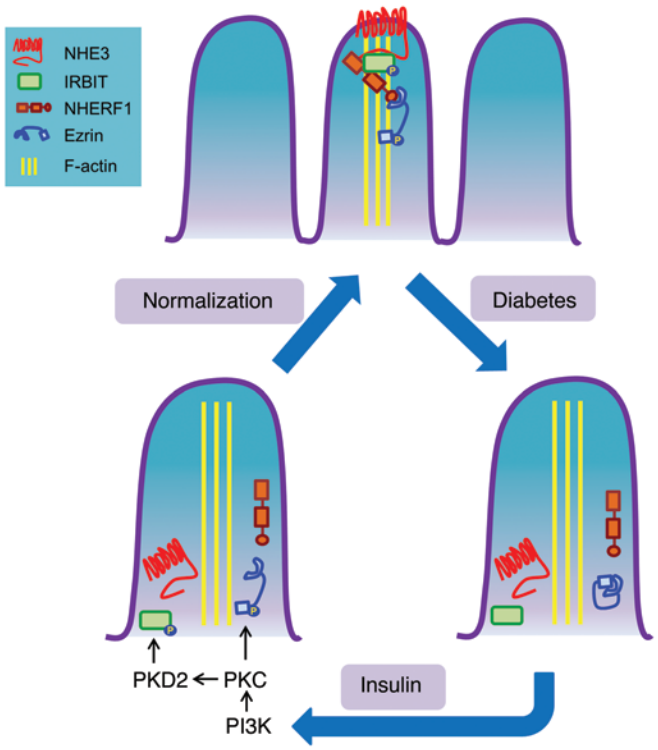

Figure 8. A model of NHE3 regulation in diabetes. NHE3 is retained in the intestinal BBM through its interaction with IRBIT, NHERF1, and ezrin under normal conditions. In diabetes, IRBIT, NHERF1, and ezrin dissociate from NHE3, resulting in loss of NHE3 from multiprotein complexes in the BBM. Insulin stimulates PI3K and PKC, which in turn activates PKD2. Active PKD2 phosphorylates IRBIT. Phosphorylated IRBIT functions a scaffold recruiting NHE3 and NHERF1 together. PKC activated by insulin phosphorylates and activates ezrin, allowing its interaction with NHERF1. NHE3 then moves as a multiprotein complex toward the tip of the microvilli, possibly aided by ezrin-mediated cytoskeleton remodeling. The dissociation of macrocomplexes consisting of NHE3, IRBIT, NHERF1, and ezrin and insulin-mediated reassembly of the complexes highlight the underlying cause of diarrhea associated with diabetes.

in DM mice by orally administering LPA for 5 days. DM mice given LPA showed an approximately 100% increase in intestinal fluid absorption compared with vehicle-treated mice (Figure 7A). Likewise, NHE3 activity was significantly enhanced in LPA-treated mice (Figure 7B). Similar to insulin, LPA corrected NHE3 localization by translocating it to the BBM (Figure 7C). To determine whether LPA- and insulin-dependent stimulation of NHE3 works through the same pathway, we examined whether knockdown of IRBIT affects NHE3 stimulation by LPA. We found that IRBIT knockdown did not attenuate the effect of LPA on NHE3 in SK-CO15 cells (Figure 7D), suggesting that insulin and LPA use different pathways. To further demonstrate the independent regulation of NHE3 by LPA and insulin, we treated DM mice with insulin, LPA, or both for 5 days. The rate of fluid absorption was higher in mice that received both LPA and insulin than in those received insulin or LPA alone (Figure 7E). Consistently, NHE3 activity in Caco-2bbe/NHE3/HA-IRBIT cells treated with the combination of insulin and LPA was significantly greater compared with single treatment with insulin or LPA (Figure 7F). These findings demonstrate that LPA and insulin independently activate NHE3 and fluid absorption in the intestine.

Discussion

In the current study, we show that decreased expression of NHE3 is associated with aberrant fluid absorption in diabetes and the restoration of fluid absorption involves a coordinated assembly of multiprotein complexes. Our study indicates that the formation of multicomplexes composed of NHE3, NHERF1, IRBIT, and ezrin provides the platform for the proper fluid absorption process in the intestine. The signaling pathways and the relative interaction are depicted in Figure 8. Diabetes results in dissociation of the multiprotein complexes, resulting in NHE3 retrieval from the BBM or failure of NHE3 delivery to the BBM. Insulin stimulates phosphorylation of IRBIT and ezrin via the PI3K/PKC/PKD2 signaling pathway. IRBIT plays a central role as a scaffold in the interaction between NHE3 and NHERF1, which mobilizes NHE3 toward the tip of the microvilli. The restoration of fluid absorption by activation of NHE3 by insulin or LPA indicates that NHE3 can act as a therapeutic target for the treatment of impaired fluid absorption in diabetes.

The mechanisms underlying diabetes-associated diarrhea are complex and poorly understood. It has been proposed that autonomic neuropathy and bacterial overgrowth contribute to diarrhea (2). Chang et al. (5) have suggested that impaired adrenergic signaling is responsible for decreased Na^+ and fluid absorption using a diabetic rat model. Electrolyte absorption and secretion are essential for maintenance of gastrointestinal fluid balance, and, hence, we attempted to understand whether BBM expression of major ion transporters and channels is altered in a rodent model of T1DM. However, the major electrolyte transporters and channels were not detected at all or detected at low frequencies by the proteomic analysis. DRA and CFTR expression, which was detected at relatively low levels, was not significantly altered in diabetic mice. The inability to detect NHE3 by mass spectrometry was puzzling, despite NHE3 enrichment in the BBMVs, but NHE3 was either not found or exhibited at a low level in previous proteomic analyses of intestinal BBMVs (34, 35). One potential reason for the absence of NHE3 is that NHE3 protein contains substantially hydrophobic regions or fewer soluble domains, which decrease the yield of trypsin-friendly proteotypic peptides for convenient protein identification (36). Nevertheless, we observed decreased NHE3 expression in diabetic mice and humans.

The current study shows that STZ-induced diabetes altered BBM expression of NHERF proteins. The changes in the expression of NHERF1 and NHERF2 but not NHERF3 were reversed by insulin. It has been shown that basal NHE3 activity is reduced in *Nherf1*$^{-/-}$ or *Nherf3*$^{-/-}$ mouse intestines (17, 37), suggesting that NHERF1 and NHERF3 may be involved in the basal expression of NHE3 at the plasma membrane. Loss of NHERF1 in mice or knockdown of NHERF1 in Caco-2bbe cells ablated insulin-mediated NHE3 activation, indicating that NHERF1 is indispensable for NHE3 regulation. NHERF1 was identified as the first regulatory pro-

tein associated with NHE3 and was shown to directly interact with NHE3 (20). However, the interaction between NHE3 and NHERF1 was weak and insufficient to coordinate NHE3 activation. We found that IRBIT is essential for the robust interaction between NHE3 and NHERF1, suggesting that NHERF1 interacts with NHE3 indirectly via IRBIT. IRBIT contains a class II PDZ ligand motif (^{527}YYRY^{530}), but whether the interaction between IRBIT, NHE3, and NHERF1 is mediated by PDZ domains remains to be determined.

Ezrin is an actin cytoskeleton-plasma membrane linker that participates in the formation of specialized domains of the BBM in IECs. Ezrin interacts with NHE3 directly or indirectly through NHERF family proteins (38–40). NHERF-mediated ezrin interaction is necessary for endocytic trafficking of NHE3, especially in the inhibition of NHE3 by cAMP (38, 39). Direct ezrin binding to NHE3, on the other hand, controls the basal NHE3 activity by regulating plasma membrane delivery of newly synthesized NHE3 and mobility of NHE3 in BBM (40). Phosphorylation of ezrin at Thr567 is also associated with vectorial translocation of NHE3 after initial activation of the Na^+-glucose cotransporter, although it is not known if this involves direct or indirect binding of ezrin to NHE3 (41). NHERF1 knockdown attenuated NHE3 and ezrin coimmunoprecipitation, suggesting that ezrin indirectly interacts with NHE3. In DM mice, the presence of ezrin in the NHE3-containing macrocomplexes was lost. The dependence of NHE3 tracking on the presence of ezrin in the multiprotein complexes is in general consistent with the previous finding that NHE3 apical targeting requires the actin cytoskeleton (42).

The finding that NHE3, IRBIT, NHERF1, and ezrin are present in 400-kDa and 500-kDa macrocomplexes is consistent with a finding from a previous study that NHE3 is present in an approximately 400-kDa complex in rabbit ileum (43). Thus, the interaction among NHE3, IRBIT, NHERF1, and ezrin forms the basis of macrocomplex assembly and NHE3-mediated absorptive process. It remains to be determined how diabetes leads to reduced BBM expression of IRBIT, NHERF1, and ezrin and their dissociation from NHE3. It was shown that activation of atypical PKC by insulin is required for insulin-stimulated glucose transport (25). Similarly, we found that phosphorylation of ezrin and IRBIT is dependent on a PKC-dependent pathway, suggesting that decreased PKC signaling causes NHE3 downregulation. However, previous studies have shown that PKC is often activated under diabetic conditions (44, 45). IECs express at least 10 isoforms of PKC, including α, βI, βII, δ, ε, and ζ (46), and PKCα is an inhibitory regulator of NHE3 (47, 48). Interestingly, our proteomics data (Supplemental Figure 1A) revealed increased expression of PKCα and PKCδ in the BBMs of diabetic mice, whereas PKCβ and PKCζ expression was decreased. These findings suggest that perturbation of specific PKC signaling may contribute to altered NHE3 expression. Another potential factor that may alter NHE3 expression is proinflammatory cytokines. Autoimmune diseases, including T1DM, are thought to involve chronic inflammation that raises levels of cytokines, nitric oxide, and free radicals (49, 50). Expression of NHE3, NHERF, and ezrin is negatively regulated by proinflammatory cytokines, such as TNF-α and IFN-γ, or loss of antiinflammatory cytokine IL-10 (51–53). Hence, future studies should determine the effect of a specific PKC isoform and cytokines on the assembly of NHE3 scaffold proteins.

LPA mediates multiple cellular responses, including cell proliferation, migration, and survival (54). Although the importance of LPA to diabetes has not been investigated extensively, LPA has been shown to improve the diabetes-induced endothelial dysfunction (55). It was reported recently that LPA stimulates glucose uptake by skeletal muscle and adipocytes and shows glucose-lowering effects in STZ-treated mice (56). Moreover, diabetic retinopathy is associated with resistance to LPA-mediated regression of retinal neovessels (57). The current study demonstrates that orally delivered LPA stimulates NHE3 and fluid absorption in diabetic mice. The effect of LPA in the absence of IRBIT and the additive nature of LPA and insulin show that LPA regulates NHE3 independent of insulin. Moreover, the apical targeting of NHE3 by both insulin and LPA suggests that NHE3 trafficking uses multiple pathways and mechanisms. Clonidine, a α2-adrenergic receptor agonist, shows some success in improving diarrhea symptoms in diabetic patients, but significant side effects limited its use as an antidiarrheal agent (5, 58). Our study provides a proof of principle that LPA has the potential to stimulate Na^+ and water absorption in T1DM. In addition to the cellular generation, LPA is present in significant amounts in several types of foodstuffs, including eggs, soybeans, and cabbage leaves (59), and future studies to test whether LPA-rich foods alleviate diabetes-associated diarrhea would be worthy. Although it is tempting to suggest that LPA or LPA-rich foods can be used as alternative therapy for diabetic patients with frequent diarrhea, this should be approached with caution, since the roots of diabetes-associated diarrheal may be complex and the biology of LPA is incompletely understood.

In summary, we have shown that diabetic mice exhibit aberrant electrolyte and fluid absorption, which in part is caused by decreased NHE3 activity in the intestine. Insulin enhances fluid absorption by restoring the BBM localization and transport activity of NHE3 in diabetic mice. NHE3 activation by insulin requires IRBIT, NHERF1, and ezrin to incorporate NHE3 in macromolecular complexes that form the physical basis for NHE3 trafficking to the BBM of IECs.

Methods

Antibodies and plasmid constructs. The following antibodies were used: mouse anti-ezrin, mouse anti–β-actin, and rabbit anti-VSVG (E8897, A1978, and V4888, respectively, Sigma-Aldrich); rabbit anti-ezrin, rabbit anti–β-tubulin, rabbit anti–phospho-ezrin, and rabbit anti-HA (3145, 2146, 3141, and 3724, respectively, Cell Signaling); mouse anti-HA (MMS-101P, Covance); mouse anti-villin (610358, BD Biosciences); mouse anti-IRBIT (H00010768-M05, Abnova); mouse anti-phosphoserine and mouse anti-NHERF (Ab6639 and Ab9526, respectively, Abcam); mouse anti-GFP (11814460001, Roche); rabbit anti-PKD2 (A300-073A, Bethyl Laboratories); rabbit anti–p-PKD2 (07-385, Millipore); and rabbit anti-NHE3 (NHE31-A, Alpha Diagnostics). We have previously described generation of the following antibodies: rabbit anti-NHE3, EM450 (32); rabbit anti-NHERF1, Ab5199 (39); rabbit anti-NHERF2, Ab5270 (39); and rabbit anti-IRBIT, EM368 (13). Mouse anti-VSVG antibody P5D4 was described previously (60). Rabbit anti-NHERF3 antibody was a gift from A.P. Naren (Cincinnati Children's Hospital, Cincinnati, Ohio, USA). Mouse anti-CFTR antibody (Ab217) was obtained from the University of North Carolina at Chapel Hill, Chapel Hill, North Carolina, USA. Plasmid constructs carrying NHE3, IRBIT, or LPA_5

were described previously (11, 13). pLKO.1 vector harboring shIRBIT, shNHERF1, shNHERF2, or shPKD2 was from Sigma-Aldrich. pcDNA3.1/CFP-NHERF1 construct was a gift from A. Newton (UCSD, San Diego, California, USA). Adenoviruses expressing CFP-ezrin and CFP-ezrin-T567A) were described previously (61).

Cell culture. Caco-2bbe and SK-CO15 cells were obtained from C. Parkos at Emory University, Atlanta, Georgia, USA, and E. Rodriguez-Boulan at Weill Medical College, Cornell University, Ithaca, New York, USA, respectively. Caco-2bbe/NHE3V and SK-CO15 cells were cultured as previously described (32). Cells were grown on Transwell filters (Corning) for 5 to 7 days after confluence to ensure differentiation prior to all assays. Where indicated, cells were treated with 100 nM insulin or 1 μM LPA.

Animals. Induction of T1DM in CF-1 male 8-week-old mice was performed by administering STZ (50 mg/kg body weight, i.p.) for 5 consecutive days. Blood glucose levels were measured biweekly, and mice with fasting glucose levels between 300 and 400 mg/dl were chosen for study. Mice were studied 3 months after STZ treatment. NHERF1-null (*Nherf1*$^{-/-}$) mice and NHERF2-null (*Nherf2*$^{-/-}$) mice were previously described (11, 62). Where indicated, mice were given Humulin-R insulin (Eli Lilly, 5 U/kg body weight, i.p.) or 0.9% NaCl as control once or daily for 5 days. LPA at 20 μM or PBS was given through gavage in 200 μl for 5 consecutive days. For all experiments with WT, *Nherf1*$^{-/-}$, and *Nherf2*$^{-/-}$ mice, male animals at the age of 3 to 4 months were used.

Patients. Preoperative medical records were reviewed for documented history of type 1 diabetes. Ileum biopsy samples were obtained from diabetic patients at Emory University Hospital (Atlanta, Georgia, USA) and VA Medical Center (Decatur, Georgia, USA) as previously described (63). Control ilea from autopsy donors were obtained from the National Development and Research Institutes. Supplemental Table 2 summarizes the subject information related to the study.

Intestinal water flux measurement. Fluid absorption measurement in the intestine was performed as described previously (11). An approximately 5-cm loop of the ileum (between 5–10 cm upstream of cecum) cannulated at the proximal and distal ends was flushed with saline for 10 minutes. This was followed by perfusion of prewarmed perfusion solution (118.4 mM NaCl, 4.7 mM KCl, 2.52 mM $CaCl_2$, 1.18 mM $MgSO_4$, 25 mM Na gluconate, 1.18 mM KH_2PO_4, pH 7.4) at 1 ml/min for 2 hours. The total amount of fluid absorption was calculated as the difference in solution volume in a reservoir from the start to the end of 2-hour perfusion.

Na^+-dependent intracellular pH recovery. Isolation of villi from mouse ileum was performed as previously described (64). In brief, mice were euthanized with isoflurane, and the ilea were flushed with cold PBS to remove food particles. An equivalent segment of the proximal ileum (approximately 10 cm upstream of the cecum) was opened longitudinally and stabilized on a cooled stage. The villi were dissected under stereomicroscope using sharpened microdissection scissors. Isolated villi were mounted on coverslips and covered with light- and solution-penetrable polycarbonate membrane (GE). The Na^+-dependent changes in intracellular pH (pH_i) of isolated villi were determined using the ratio-fluorometric 2′,7′-bis-(2-carboxyethyl)-5-carboxyfluorescein acetoxymethyl ester (BCECF-AM) (Sigma-Aldrich) (excitation at 495 nm and 440 nm; emission at 530 nm) as described previously (65). Comparisons of Na^+/H^+ exchange were made between measurements done on the same day.

BBMV preparation. Preparation of BBMVs from the mouse intestinal epithelia was performed as previously described (34).

Coimmunoprecipitation and Western blot. Cell lysate preparation, immunoprecipitation, and Western blotting were performed as described (19). Densitometric analysis was performed using ImageJ software (NIH).

BN-PAGE. BBMVs prepared from ileal scrapes were solubilized for 30 minutes in 1 × native lysis buffer supplemented with 2% dodecylmaltoside (Life Technologies). Ten μg protein was separated on a 4% to 16% NativePAGE Novex gel using Coomassie G250 as a charge-shift molecule. At the end of the electrophoresis, the gel was removed and equilibrated for 60 minutes in an equilibration buffer (PBS containing 1% [w/v] SDS and 1% [w/v] β-mercaptoethanol) with gentle agitation. Protein transfer from BN-PAGE gels onto PVDF membranes was carried out in a regular transfer buffer. Membranes were rinsed twice in methanol and once in H_2O to remove G250 dye prior to immunoblotting.

Surface biotinylation. Surface biotinylation of NHE3 was performed as previously described (13). Caco-2bbe/NHE3V or SK-CO15 cells were incubated for 40 minutes with 0.5 mg/ml NHS-SS-biotin in borate buffer and lysed. An aliquot was retained as the total fraction representing the total cellular NHE3. One mg of lysate was incubated with streptavidin-agarose beads (Thermo), and biotinylated surface proteins representing surface NHE3 were then eluted. Densitometric analysis was performed using ImageJ software.

Confocal immunofluorescence microscopy and PLA. Human biopsies were formalin-fixed, paraffin-embedded, and cut into 5-μm sections. Sections were deparaffinized and rehydrated, and antigen unmasking was performed through pressure cooker treatment in sodium citrate buffer (10 mM sodium citrate, 0.05% Tween 20, pH 6.0). For rodents, 2-cm segments of the proximal ilea were fixed with 4% paraformaldehyde and fixed in OCT compound and sectioned into 6-μm thick sections. Caco-2bbe cells grown on Transwell filters to support differentiation were fixed with 4% PFA. The fluorescence staining procedures were described previously (64). Specimens were observed under a Zeiss LSM510 laser confocal microscope (Zeiss). In situ PLA was carried out with the Duolink Detection Kit (Bethyl Laboratories). Briefly, permeabilized cells were incubated with primary antibody at room temperature. After washes, cells were incubated with appropriate PLA oligonucleotide probes conjugated with anti-mouse or anti-rabbit secondary antibody. Circularization and ligation was performed in ligase-containing solution for 30 minutes at 37°C, followed by amplification with complementary probes labeled with Alexa Fluor 554. Cells were next incubated with Alexa Fluor 488–conjugated phalloidin. Fluorescence images were taken using a Zeiss LSM510 laser confocal microscope with ×63 Pan-Apochromat oil lenses. Quantification of PLA signal was carried out by counting the number of red signals on a minimum of 50 representative cells.

Quantitative RT-PCR. For details regarding quantitative RT-PCR methods and primer sequences, see the Supplemental Methods.

Mass spectrometry proteomics data. The mass spectrometry proteomics data have been deposited to the ProteomeXchange Consortium via the PRIDE partner repository with the data set identifiers PXD001859 and 10.6019/PXD001859.

Statistics. Statistical significance was assessed by a 2-tailed unpaired Student's *t* test. Results are presented as mean ± SEM. A *P* value of less than 0.05 was considered significant.

Study approval. The study with human patients was approved by the Institutional Review Board Committees at Emory University and the Atlanta VA Medical Center. Animals were maintained and experiments were performed with the approval of the Institutional Animal Care and Use Committee of Emory University.

Acknowledgments

This work was supported by NIH grants DK061418 (to C. Yun) and DK080684 (to S. Srinivasan), VA Merit Awards BX000136 (to S. Srinivasan) and BX002540 (to C. Yun), and American Heart Association Scientist Development Grant 13SDG1623001 (to P. He). The microscopy core was supported by R24DK064399.

Address correspondence to: C. Chris Yun, Division of Digestive Diseases, Department of Medicine, Emory University School of Medicine, Whitehead Research Bldg. Room 201, 615 Michael Street, Atlanta, Georgia 30322, USA. Phone: 404.712.2865; E-mail: ccyun@emory.edu.

1. Gould M, Sellin JH. Diabetic diarrhea. *Curr Gastroenterol Rep*. 2009;11(5):354–359.
2. Ogbonnaya KI, Arem R. Diabetic diarrhea. Pathophysiology, diagnosis, and management. *Arch Intern Med*. 1990;150(2):262–267.
3. Miller LJ. Small intestinal manifestations of diabetes mellitus. *Yale J Biol Med*. 1983;56(3):189–193.
4. Virally-Monod M, et al. Chronic diarrhoea and diabetes mellitus: prevalence of small intestinal bacterial overgrowth. *Diabetes Metab*. 1998;24(6):530–536.
5. Chang EB, Bergenstal RM, Field M. Diarrhea in streptozocin-treated rats. Loss of adrenergic regulation of intestinal fluid and electrolyte transport. *J Clin Invest*. 1985;75(5):1666–1670.
6. Field M. Intestinal ion transport and the pathophysiology of diarrhea. *J Clin Invest*. 2003;111(7):931–943.
7. Hoglund P, Haila S, Socha J, Tomaszewski L, Saarialho-Kere U, et al. Mutations of the down-regulated in adenoma (DRA) gene cause congenital chloride diarrhoea. *Nat Genet*. 1996;14(3):316–319.
8. Schultheis PJ, et al. Renal and intestinal absorptive defects in mice lacking the NHE3 Na^+/H^+ exchanger. *Nat Genet*. 1998;19(3):282–285.
9. Welsh MJ, Smith AE. Molecular mechanisms of CFTR chloride channel dysfunction in cystic fibrosis. *Cell*. 1993;73(7):1251–1254.
10. Barrett KE, Keely SJ. Chloride secretion by the intestinal epithelium: molecular basis and regulatory aspects. *Annu Rev Physiol*. 2000;62:535–572.
11. Lin S, et al. Lysophosphatidic acid stimulates the intestinal brush border Na(+)/H(+) exchanger 3 and fluid absorption via LPA(5) and NHERF2. *Gastroenterology*. 2010;138(2):649–658.
12. Seidler U, et al. The role of the NHERF family of PDZ scaffolding proteins in the regulation of salt and water transport. *Ann N Y Acad Sci*. 2009;1165:249–260.
13. He P, Zhang H, Yun CC. IRBIT, inositol 1,4,5-triphosphate (IP3) receptor-binding protein released with IP3, binds Na^+/H^+ exchanger NHE3 and activates NHE3 activity in response to calcium. *J Biol Chem*. 2008;283(48):33544–33553.
14. Fuster DG, Bobulescu IA, Zhang J, Wade J, Moe OW. Characterization of the regulation of renal Na^+/H^+ exchanger NHE3 by insulin. *Am J Physiol Renal Physiol*. 2007;292(2):F577–F585.
15. Klisic J, et al. Insulin activates Na(+)/H(+) exchanger 3: biphasic response and glucocorticoid dependence. *Am J Physiol Renal Physiol*. 2002;283(3):F532–F539.
16. Zachos NC, Tse M, Donowitz M. Molecular physiology of intestinal Na^+/H^+ exchange. *Annu Rev Physiol*. 2005;67:411–443.
17. Broere N, et al. Defective jejunal and colonic salt absorption and altered Na(+)/H (+) exchanger 3 (NHE3) activity in NHE regulatory factor 1 (NHERF1) adaptor protein-deficient mice. *Pflugers Arch*. 2009;457(5):1079–1091.
18. Yoo BK, He P, Lee SJ, Yun CC. Lysophosphatidic acid 5 receptor induces activation of Na(+)/H(+) exchanger 3 via apical epidermal growth factor receptor in intestinal epithelial cells. *Am J Physiol Cell Physiol*. 2011;301(5):C1008–C1016.
19. He P, Klein J, Yun CC. Activation of Na^+/H^+ exchanger NHE3 by angiotensin II is mediated by inositol 1,4,5-triphosphate (IP3) receptor-binding protein released with IP3 (IRBIT) and Ca^{2+}/calmodulin-dependent protein kinase II. *J Biol Chem*. 2010;285(36):27869–27878.
20. Weinman EJ, et al. A C-terminal PDZ motif in NHE3 binds NHERF-1 and enhances cAMP inhibition of sodium-hydrogen exchange. *Biochemistry*. 2003;42(43):12662–12668.
21. Ando H, et al. IRBIT suppresses IP3 receptor activity by competing with IP3 for the common binding site on the IP3 receptor. *Mol Cell*. 2006;22(6):795–806.
22. Ando H, Mizutani A, Matsu-ura T, Mikoshiba K. IRBIT, a novel inositol 1,4,5-trisphosphate (IP3) receptor-binding protein, is released from the IP3 receptor upon IP3 binding to the receptor. *J Biol Chem*. 2003;278(12):10602–10612.
23. Shirakabe K, et al. IRBIT, an inositol 1,4,5-trisphosphate receptor-binding protein, specifically binds to and activates pancreas-type $Na^+/HCO3^-$ cotransporter 1 (pNBC1). *Proc Natl Acad Sci U S A*. 2006;103(25):9542–9547.
24. Rozengurt E. Protein kinase D signaling: multiple biological functions in health and disease. *Physiology (Bethesda)*. 2011;26(1):23–33.
25. Farese RV, Sajan MP, Standaert ML. Atypical protein kinase C in insulin action and insulin resistance. *Biochem Soc Trans*. 2005;33(pt 2):350–353.
26. Chiu TT, Leung WY, Moyer MP, Strieter RM, Rozengurt E. Protein kinase D2 mediates lysophosphatidic acid-induced interleukin 8 production in nontransformed human colonic epithelial cells through NF-κB. *Am J Physiol Cell Physiol*. 2007;292(2):C767–C777.
27. Weinman EJ, et al. Cooperativity between the phosphorylation of Thr95 and Ser77 of NHERF-1 in the hormonal regulation of renal phosphate transport. *J Biol Chem*. 2010;285(33):25134–25138.
28. Algrain M, Turunen O, Vaheri A, Louvard D, Arpin M. Ezrin contains cytoskeleton and membrane binding domains accounting for its proposed role as a membrane-cytoskeletal linker. *J Cell Biol*. 1993;120(1):129–139.
29. Matsui T, et al. Rho-kinase phosphorylates COOH-terminal threonines of ezrin/radixin/moesin (ERM) proteins and regulates their head-to-tail association. *J Cell Biol*. 1998;140(3):647–657.
30. Cha B, Donowitz M. The epithelial brush border Na^+/H^+ exchanger NHE3 associates with the actin cytoskeleton by binding to ezrin directly and via PDZ domain-containing Na^+/H^+ exchanger regulatory factor (NHERF) proteins. *Clin Exp Pharmacol Physiol*. 2008; 35(8):863–871.
31. Yung YC, Stoddard NC, Chun J. LPA receptor signaling: pharmacology, physiology, and pathophysiology. *J Lipid Res*. 2014;55(7):1192–1214.
32. Yoo BK, Yanda MK, No YR, Yun CC. Human intestinal epithelial cell line SK-CO15 is a new model system to study Na(+)/H(+) exchanger 3. *Am J Physiol Gastrointest Liver Physiol*. 2012;303(2):G180–G188.
33. No YR, He P, Yoo BK, Yun CC. Regulation of NHE3 by lysophosphatidic acid is mediated by phosphorylation of NHE3 by RSK2. *Am J Physiol Cell Physiol*. 2015;309(1):C14–C21.
34. Donowitz M, et al. Proteome of murine jejunal brush border membrane vesicles. *J Proteome Res*. 2007;6(10):4068–4079.
35. McConnell RE, Benesh AE, Mao S, Tabb DL, Tyska MJ. Proteomic analysis of the enterocyte brush border. *Am J Physiol Gastrointest Liver Physiol*. 2011;300(5):G914–G926.
36. Whitelegge JP. Integral membrane proteins and bilayer proteomics. *Anal Chem*. 2013;85(5):2558–2568.
37. Hillesheim J, et al. Down regulation of small intestinal ion transport in PDZK1- (CAP70/ NHERF3) deficient mice. *Pflugers Arch*. 2007;454(4):575–586.
38. Yun CH, et al. cAMP-mediated inhibition of the epithelial brush border Na^+/H^+ exchanger, NHE3, requires an associated regulatory protein. *Proc Natl Acad Sci U S A*. 1997;94(7):3010–3015.
39. Yun CH, Lamprecht G, Forster DV, Sidor A. NHE3 kinase A regulatory protein E3KARP binds the epithelial brush border Na^+/H^+ exchanger NHE3 and the cytoskeletal protein ezrin. *J Biol Chem*. 1998;273(40):25856–25863.
40. Cha B, et al. The NHE3 juxtamembrane cytoplasmic domain directly binds ezrin: dual role in NHE3 trafficking and mobility in the brush border. *Mol Biol Cell*. 2006;17(6):2661–2673.
41. Zhao H, et al. Ezrin regulates NHE3 translocation and activation after Na^+-glucose cotransport. *Proc Natl Acad Sci U S A*. 2004;101(25):9485–9490.
42. Kurashima K, et al. The apical Na(+)/H(+)

exchanger isoform NHE3 is regulated by the actin cytoskeleton. *J Biol Chem*. 1999;274(42):29843–29849.
43. Li X, et al. Carbachol regulation of rabbit ileal brush border Na^+-H^+ exchanger 3 (NHE3) occurs through changes in NHE3 trafficking and complex formation and is Src dependent. *J Physiol*. 2004;556(pt 3):791–804.
44. Noh H, King GL. The role of protein kinase C activation in diabetic nephropathy. *Kidney Int*. 2007;(106):S49–S53.
45. Geraldes P, King GL. Activation of protein kinase C isoforms and its impact on diabetic complications. *Circ Res*. 2010;106(8):1319–1331.
46. Farhadi A, Keshavarzian A, Ranjbaran Z, Fields JZ, Banan A. Th e role of protein kinase C isoforms in modulating injury and repair of the intestinal barrier. *J Pharmacol Exp Ther*. 2006;316(1):1–7.
47. Clayburgh DR, Musch MW, Leitges M, Fu YX, Turner JR. Coordinated epithelial NHE3 inhibition and barrier dysfunction are required for TNF-mediated diarrhea in vivo. *J Clin Invest*. 2006;116(10):2682–2694.
48. Lee-Kwon W, et al. Ca^{2+}-dependent inhibition of NHE3 requires PKC alpha which binds to E3KARP to decrease surface NHE3 containing plasma membrane complexes. *Am J Physiol Cell Physiol*. 2003;285(6):C1527–C1536.
49. Christen U, et al. A dual role for TNF-α in type 1 diabetes: islet-specific expression abrogates the ongoing autoimmune process when induced late but not early during pathogenesis. *J Immunol*. 2001;166(12):7023–7032.
50. Goldberg RB. Cytokine and cytokine-like inflammation markers, endothelial dysfunction, and imbalanced coagulation in development of diabetes and its complications. *J Clin Endocrinol Metab*. 2009;94(9):3171–3182.
51. Jiang WG, Hiscox S. Cytokine regulation of ezrin expression in the human colon cancer cell line HT29. *Anticancer Res*. 1996;16(2):861–865.
52. Lenzen H, et al. Downregulation of the NHE3-binding PDZ-adaptor protein PDZK1 expression during cytokine-induced inflammation in interleukin-10-deficient mice. *PLoS One*. 2012;7(7):e40657.
53. Amin MR, Malakooti J, Sandoval R, Dudeja PK, Ramaswamy K. IFN-γ and TNF-α regulate human NHE3 gene expression by modulating the Sp family transcription factors in human intestinal epithelial cell line C2BBe1. *Am J Physiol Cell Physiol*. 2006;291(5):C887–C896.
54. van Meeteren LA, Moolenaar WH. Regulation and biological activities of the autotaxin-LPA axis. *Prog Lipid Res*. 2007;46(2):145–160.
55. Cameron NE, Jack AM, Cotter MA. Effect of α-lipoic acid on vascular responses and nociception in diabetic rats. *Free Radic Biol Med*. 2001;31(1):125–135.
56. Yea K, et al. Lysophosphatidic acid regulates blood glucose by stimulating myotube and adipocyte glucose uptake. *J Mol Med (Berl)*. 2008;86(2):211–220.
57. Aranda J, Motiejunaite R, Im E, Kazlauskas A. Diabetes disrupts the response of retinal endothelial cells to the angiomodulator lysophosphatidic acid. *Diabetes*. 2012;61(5):1225–1233.
58. Fedorak RN, Field M, Chang EB. Treatment of diabetic diarrhea with clonidine. *Ann Intern Med*. 1985;102(2):197–199.
59. Tanaka T, et al. Quantification of phosphatidic acid in foodstuffs using a thin-layer-chromatography-imaging technique. *J Agric Food Chem*. 2012;60(16):4156–4161.
60. Kreis TE. Microinjected antibodies against the cytoplasmic domain of vesicular stomatitis virus glycoprotein block its transport to the cell surface. *EMBO J*. 1986;5(5):931–941.
61. Zhu L, et al. Comparative study of ezrin phosphorylation among different tissues: more is good; too much is bad. *Am J Physiol Cell Physiol*. 2008;295(1):C192–C202.
62. Shenolikar S, Voltz JW, Minkoff CM, Wade JB, Weinman EJ. Targeted disruption of the mouse NHERF-1 gene promotes internalization of proximal tubule sodium-phosphate cotransporter type IIa and renal phosphate wasting. *Proc Natl Acad Sci U S A*. 2002;99(17):11470–11475.
63. Chandrasekharan B, et al. Colonic motor dysfunction in human diabetes is associated with enteric neuronal loss and increased oxidative stress. *Neurogastroenterol Motil*. 2011;23(2):131–138.
64. He P, et al. Serum- and glucocorticoid-induced kinase 3 in recycling endosomes mediates acute activation of Na^+/H^+ exchanger NHE3 by glucocorticoids. *Mol Biol Cell*. 2011;22(20):3812–3825.
65. Wang D, Sun H, Lang F, Yun CC. Activation of NHE3 by dexamethasone requires phosphorylation of NHE3 at Ser663 by SGK1. *Am J Physiol Cell Physiol*. 2005;289(4):C802–C810.